

Mineral prospectivity mapping in GIS using fuzzy logic integration in Khondab area, western Markazi province, Iran

Morteza Tabaei^{1,*}, Mahin Mansouri Esfahani¹, Pezhman Rasekh¹, Ali Esna-ashari²

1- Department of Mining Engineering, Isfahan University of Technology, Isfahan, Iran.

2- Geological Survey of Iran

* Corresponding Author: mtabaei@cc.iut.ac.ir

Received: 22 April 2018 / Accepted: 04 September 2018 / Published online: 08 September 2018

Abstract: Khondab area is located in western Markazi province, within the Sanandaj-Sirjan Zone. The zone has been previously known to be associated with Pb, Zn, Cu, Fe, Ba and Si elements. The current study is carried out to identify new promising targets for regional exploration. Multiple data sources (e.g., magnetic surveys, faults, geological and satellite data) are processed and then integrated by using Fuzzy Logic modelling to produce a final prospectivity map for regional exploration of MVT deposits in the Khondab area. Finally, resulted prospectivity map is validated by analyzing field derived samples collected over revealed promising zones of the study area and ore-microscopic studies of the collected samples also confirmed MVT mineralization. Validation process indicates that Cretaceous limestone units are in high correlation with MVT mineralization in this area. Based on priority rating of exploration targets, the eastern and the south-eastern parts of the study area are the most promising parts for further exploration of MVT deposits.

Keywords: Fuzzy Logic modelling; Khondab area; MVT; Sanandaj-Sirjan Zone.

1- Introduction

Acquiring the pre-known exploration models and proper integration techniques to delineate new promising zones is widely recommended in mineral prospectivity mapping. There are two GIS-based integration techniques including data-driven and knowledge-driven modelling techniques. In the first case, mineralization features of the pre-known deposits are applied over the unknown ones. Some common methods of this approach are including: weight of evidence (Bonham-Carter, 1994), logistic regression (Chung and Agterburg, 1980), decision tree analysis (Reddy and Bonham-carter, 1991) and neural networks (Brown et al., 2000). The mentioned methods are applicable only if the number of the same pre-known deposits and their associated information are sufficient for further decision makings. Due to this limitation of data-driven methods, knowledge-driven methods were introduced

(Bonham-Carter, 1994). Based on these methods, different crisp values are assigned to the informative layers one after another assuming their respective relative importance toward the mineralization process. The crisp values are assigned based on the exploration expert's knowledge. Methods including Boolean logic, index overlay (Harris et al., 2001) and fuzzy logic (An et al., 1991) are classified as knowledge-driven methods. Previous studies have already demonstrated that fuzzy modelling approach within GIS environment is widely accepted among geoscience experts. The approach is widely used in exploration of iron deposits (An et al., 1991), Mississippi Valley-Type (MVT) mineralization (Eddy et al., 1995) and also epithermal gold deposits (Carranza et al., 1999). An et al. (1991) used a reclassified lithology map combined with several geophysical maps to generate a fuzzy model and

then plotting a perspective plot of base metals and iron deposits in Farley Lake exploration area located in Canada (An et al., 1991). Getingz and Bultmann (1993) used fuzzy function to plot the mineral potential map of quartz-carbonate bearing veins of southeast parts of Arizona in USA. Different crisp values are assigned to each informative layer due to the technical expert's knowledge. The resulted maps are integrated using fuzzy overlay technique to create a map of favourable areas of mineralization (Gettings et al., 1993). Karimi and Valdan Zoj (2003) created a mineral potential map of Rigan copper mineralization in the Kerman region, Iran. Cheng and Agterberg (1999) proposed weighted fuzzy models for mineral potential mapping. Carranza and Hale (2001) performed a geologically-constrained fuzzy mapping of gold mineralization. Macedon and Ara'ujo (2002) used fuzzy logic approach in creation of the favourability map associated with sulphide iron mineralization. Porwall et al. (2003) used both knowledge-driven and data-driven fuzzy approaches in creation of mineral potential maps of Sedimentary Exhalative Deposits (SEDEX) in Aravalli province (western India). Eddy et al. (2006) used fuzzy logic approach for exploration of MVT lead-zinc deposits. Eliasi et al. (2007) created a mineral potential map of Now-Chun copper deposit which made a significant progress in finding promising drill targets. Nykanen et al. (2008) used fuzzy logic approach to plot regional-scale mineral potential maps of Iron Oxide Copper Gold Deposits (IOCG) in Finland. Adeli (2009) provided mineral potential map of Chah-Firuzeh exploration area and proposed some promising drilling targets. Pazand and Hezarkhani (2018), Pazand et al. (2014) acquired a multi-criteria fuzzy logic approach within GIS environment to find out new promising zones of porphyry copper mineralization. Finally, Rasekh et al. (2016)

applied fuzzy logic data integration to locate new promising zones of copper mineralization in Kajan area, Isfahan, Iran.

The current study is theoretically similar to above-mentioned studies and includes different exploration data sets of geological map, airborne magnetometer surveys, faults and satellite data. The data are integrated by fuzzy logic data integration technique to identify special proxies related to MVT mineralization. The proxies imply promising targets of MVT mineralization in Khondab area. Different samples are also collected from the promising targets of fuzzy logic model. The samples are then studied using a polarizing microscope hosted in Department of Mining Engineering at Isfahan University of Technology. Microscopic studies of the polished and thin sections confirmed mineralization characteristics of MVT mineralization.

2- Geological Setting

The study area is located in western Markazi province, within the Sanandaj-Sirjan Zone. Rock types of the study area are divided into 10 major units. The units of the area ranges from calcareous sandstones to calcareous illitic slates. Lower-middle Jurassic units are the oldest ones composed of slates and phyllites. These units have been widely covered the west, the northwest, the southwest and the north of the area. Shemshak Formation has covered the oldest rock unit of the area and is comprised of slaty sandstone units. The formation itself is covered by lower cretaceous limestones and monzodioritic-monzonitic units. Figure 1 shows the location map of the Khondab area in the Sanandaj-Sirjan Zone and also the 1:100000 geological map of the area.

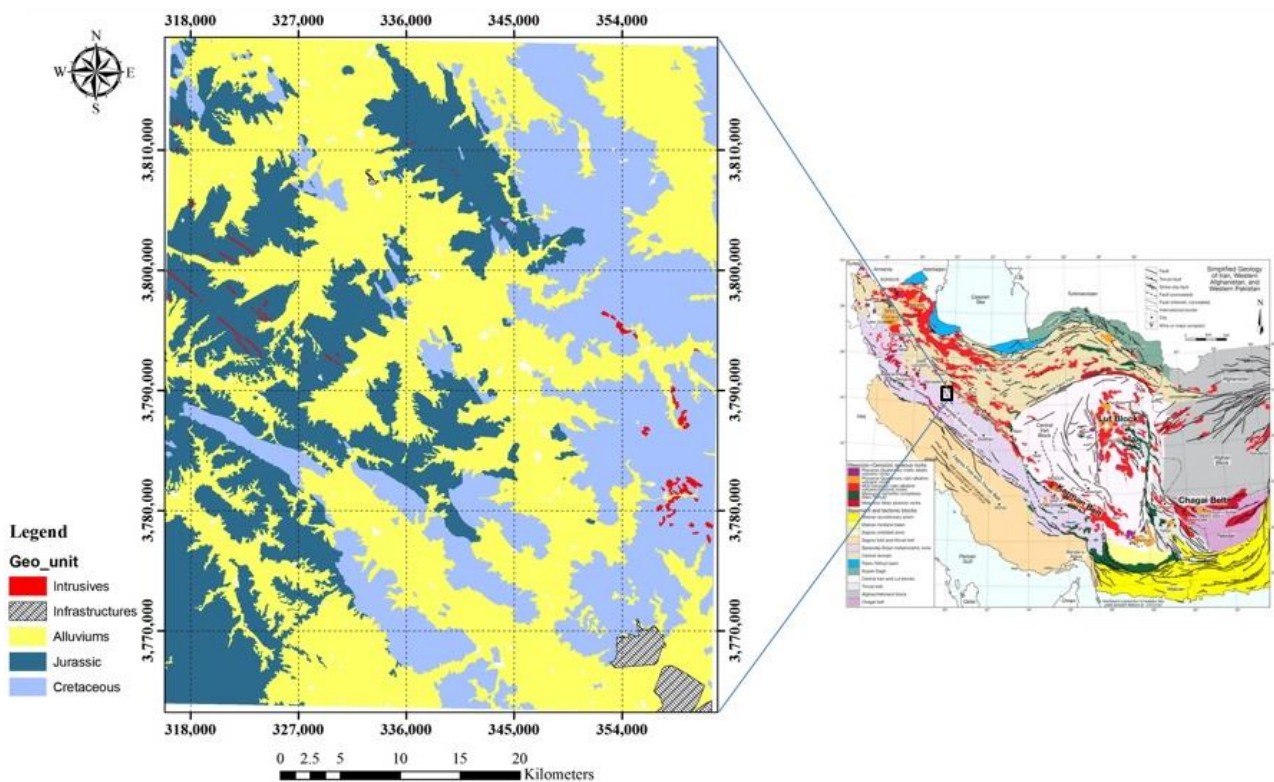


Figure 1) Simplified geological map of the Khondab area.

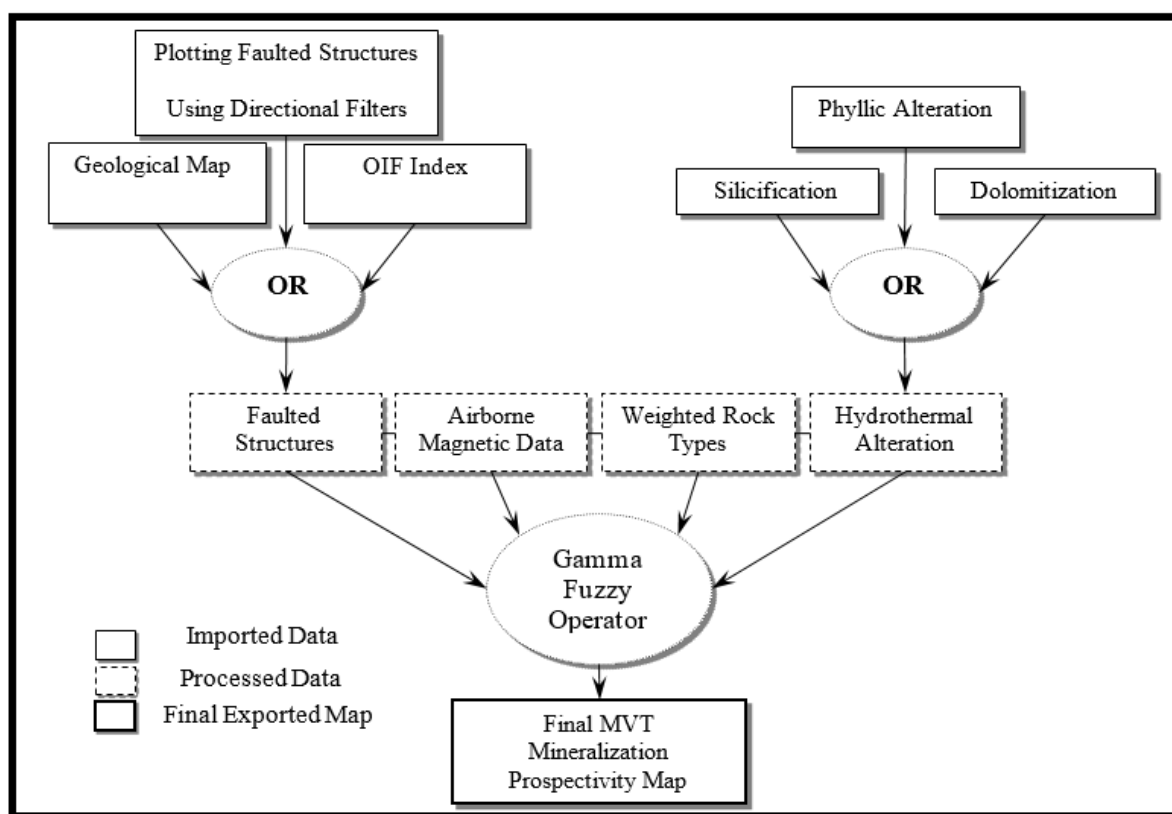


Figure 2) Schematic diagram of the fuzzy logic data integration procedure.

3- Discussion

Fuzzy logic approach is considered as a knowledge-driven modelling method. It applies membership functions (μ) and different

combinations of fuzzy operators to prepare a final weighted prospectivity map. Mathematically, a fuzzy set, A, is a set of ordered pairs (Ziaii et al., 2009):

$$A = \{(x, \mu(x)) \mid x \in X\} \quad (1)$$

Where X = collection of objects, also known as the universal set and $\mu(x)$ = membership function or degree of compatibility of x in $\mu(x)$. The range of $\mu(x)$ is $[0, 1]$; where 0 represents non-membership and 1 represents full membership. An et al. (1991) proposed that the five operators of fuzzy AND, fuzzy OR, fuzzy algebraic product, fuzzy algebraic sum and fuzzy gamma are applicable for integrating exploration datasets. The fuzzy OR takes the maximum value of any of the input maps, for any individual pixel. Meanwhile, AND operator takes the minimum value of any of the input maps, for any particular pixel. The OR operator is used where two map patterns represent the same level of evidence. The resulted combination of data sets by this operator suggests evidences at higher probabilities. Gamma operator (γ) is a combination of the fuzzy algebraic product and the fuzzy algebraic sum operators. The operator produces output values that ensure a flexible compromise between the increasing tendencies of the fuzzy algebraic sum and the decreasing effects of the fuzzy algebraic product. During the following sections, multiple datasets (aeromagnetic, faults, geological and satellite data) are processed separately (Fig. 2) and fuzzy membership value of each individual informative layer is calculated using ArcGIS fuzzy logic toolbox.

3.1- Geological data

Upper Jurassic to lower Cretaceous rock types of the study area are covered almost 52% of the surficial geologic map (The other 48% of the surface is made up of alluvial). Major rock types of the area are Jurassic sandstones and slates. Cretaceous rock units consist of calcareous sandstones, sandy limestones, dolomitic sandstones and calcareous illitic slates. Considering the significant role of intermediate plutonic bodies in MVT mineralization, we assigned them the highest crisp value (9 out of 10). These bodies are located in eastern and south-eastern parts of the study area. Intrusive

units have the key role in providing mineralization conditions such as the required heat source. Hence, intrusive units are considered as one of the important rock units and got the weight of 7 out of 10. Additionally, the weight of 3 is assigned to sandstones and Jurassic sandy slates due to their poor relationship with mineralized occurrences of the study area. Finally, alluvial and Quaternary sediments got the weight of 1 out of 10 and urban areas got the weight of 0 (Table 1). Final weighted evidence map of geological layer is shown in Figure 3.

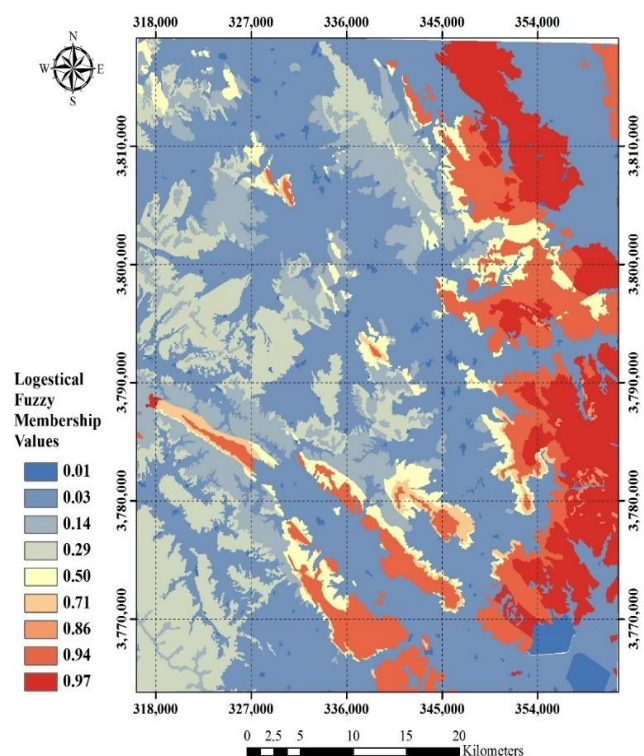


Figure 3) Weighted evidence map of rock types of the study area.

3.2- Airborne magnetic data

In this section, countrywide airborne magnetic data of Iran is used. This data is carried out in 1976 with resolution of 7.5 Km. RTP correction is done using Oasis Montaj® 4.3 geophysical software (Fig. 4). Within the map (Fig. 4), geomagnetic responses vary between -650 to +150 nT. Significant negative values are related to faults and probably wide hydrothermal alterations. Also, significant positive values are assigned to intrusive intermediate to basic

subsurface bodies. Low to intermediate values indicate sedimentary and metamorphic rocks. Based on the geomagnetic responses, evident map of airborne magnetic data is classified into 5 different classes.

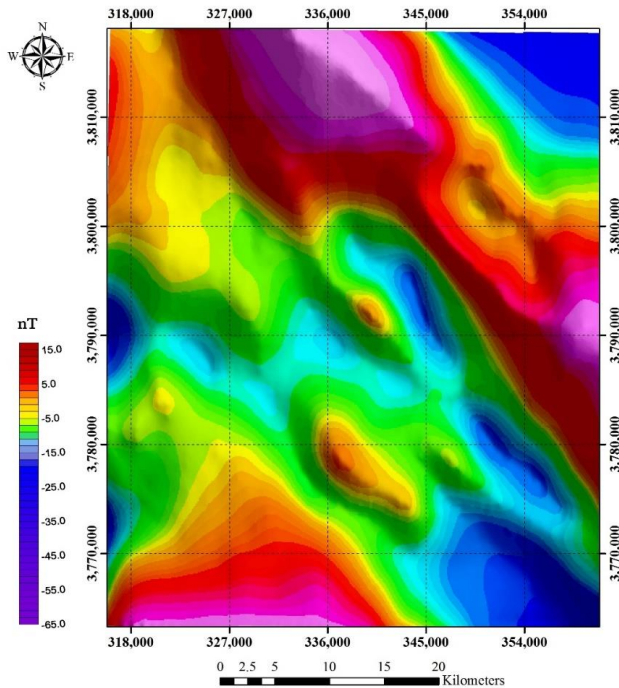


Figure 4) Figure 4. RTP map of the study area.

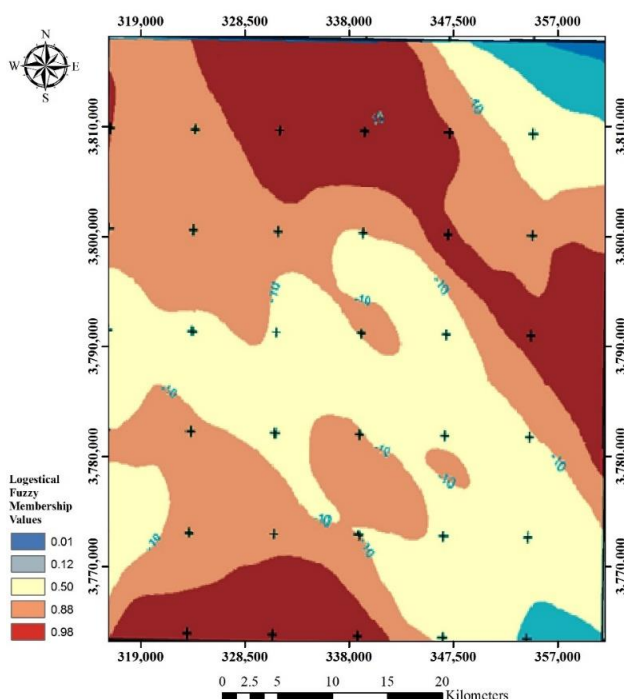


Figure 5) Reclassified geophysical map of the study area.

According to the resulted map of the airborne magnetic data, the study area is classified into three main zones. Two of them show significant

magnetic anomalies and are related to ferromagnetic minerals of the deep intermediate plutonic units. Direction of the two mentioned anomalies shows features with the same trend (NW-SE) as the promising rock types of the study area. Depletion of magnetic responses in NE and SE parts of the area are due to the widely spreading alluvial over these areas. Assuming the decisive role of plutonic bodies in preparing the required thermal source of mineralization, the weight of 7 out of 10 is considered for these bodies (Table 2). Resulted map is then reclassified into five different classes according to technical expert's knowledge (Fig. 5).

3.3- Remote sensing data

The silicification process is in high correlation with MVT mineralization. Hence, silicified zones are very important for targeting MVT mineralization. Quartz is the main mineral of silicified zones and is indicated by ASTER thermal infrared wavelength region. To delineate silicified zones, selective principal component analysis is carried out on the thermal infrared wavelength region of ASTER satellite imagery data according to Crosta technique. In Crosta Technique, the magnitude and positive/negative value of a special vector provide useful information regarding spectral characteristics of vegetarians, stones and clays. This information is projected in any PC or component. High spectral differences of the second PC is considered to be relevant to the silicified zones. Considering the significant role of residual silicified hydrothermal fluids in transporting metallic elements and consequent deposition of ore deposits, the highest weight (9 out of 10) is assigned to this type of alteration. The resulted map is then reclassified into two classes so that one of the classes specifies the qualified areas (Weight 9 out of 10) and the other one identifies non-qualified areas (weight 1 out of 10), (Table 3 and Fig. 6). Dolomitization is in high consistence with the carrying canals of ore-bearing fluids. Hence, to

target the dolomitized zones, ROWAN band ratio is used. ROWAN (2003) is introduced by USGS as follow:

$$R[S(6,8),7] \tag{2}$$

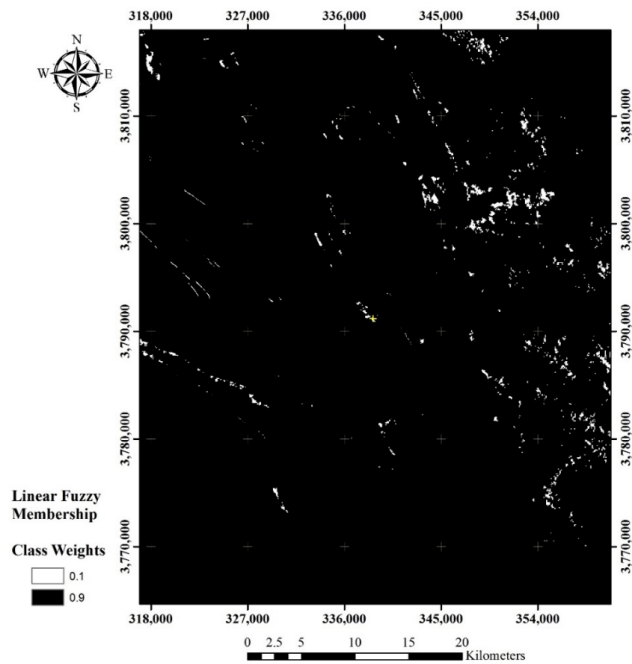


Figure 6) Silicified alteration zones of the study area.

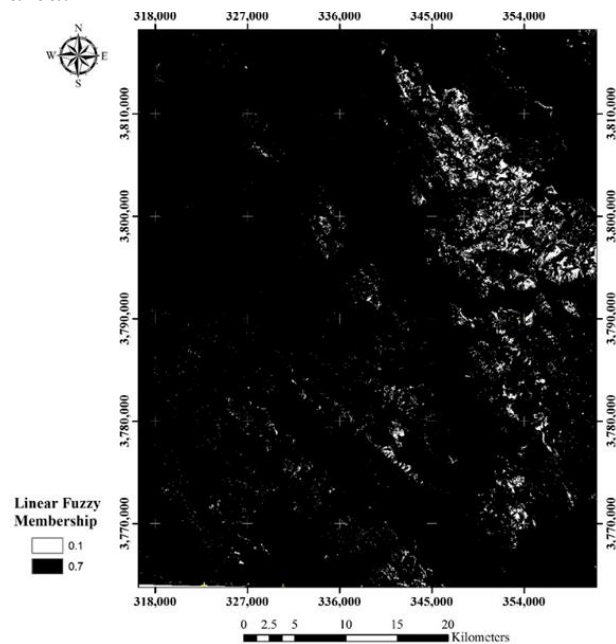


Figure 7) Dolomitized alteration zones of the study area.

Assuming the importance of dolomitization in MVT mineralization, the weight 7 out of 10 is assigned to this type of alteration (Fig. 7). Muscovite is generally considered as an indicator for phyllic alteration. To identify

phyllic alteration zones, optical absorption spectrum features of muscovite is used (Sameni, 2001). According to absorption (6th band) and reflectance (4th band) of muscovite's spectra, band ratio of 4/6 is proposed for locating muscovite in the study area. The 4th PC is then specified to be the proper one in Crosta transformation technique. Comparing with the two types of silicification and dolomitization alterations, phyllic alteration has the third position of importance in MVT mineralization.

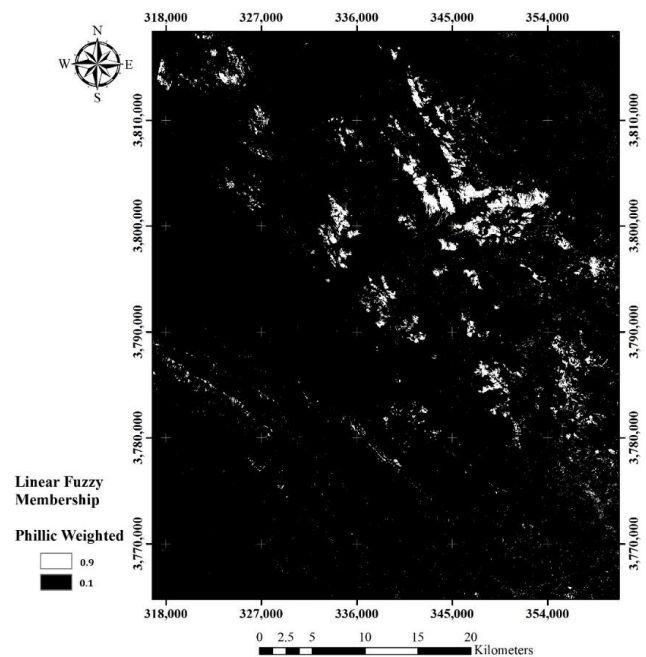


Figure 8) Phyllic alteration zones of the study area.

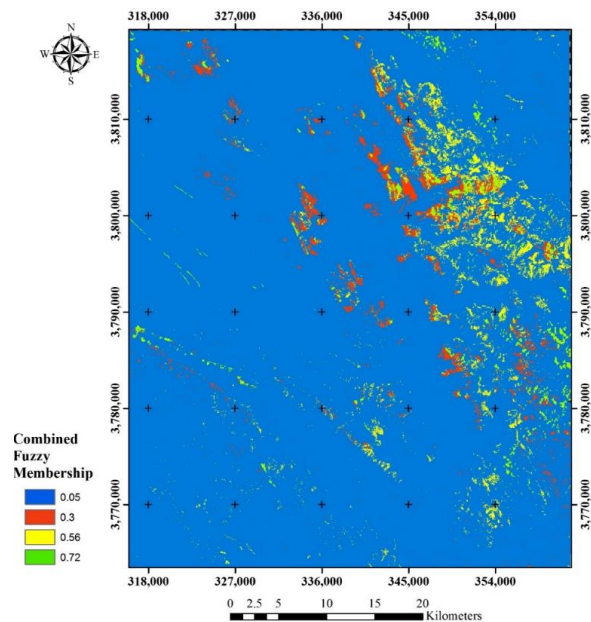


Figure 9) Final weighted map of alteration zones of Khondab area.

Hence, the weight 5 is assigned to this type of alteration (Fig. 8). After mapping the alterations, three weighted evidence maps of each alteration type are integrated by OR fuzzy operator (Table 3 and Fig. 9).

Table 1) Detailed information of lithology units.

Logistical Fuzzy Membership	Class Score	Class Weight	Class Name		Layer Weight	Evidence Map
0.71	54	6	K_2^s	Light grey illite bearing slate with intercalation of calcareous slate, biomicritic recrystallized limestone and calcareous silty slate	9	Lithology Units Evidence Map
0.94	72	8	K_1^{sl}	Brownish light grey slaty recrystallized limestone, calcareous slate and sandy slate with intercalation		
0.97	81	9	K_1^d	Greyish yellow slightly metamorphosed recrystallized Orbitolina bearing dolomitic limestone, sandy limestone and biomicritic limestone		
0.97	81	9	K_1^l	Grey thick bedded to massive slightly metamorphosed Orbitolina bearing limestone		
0.71	54	6	K_1^m	Buff thin to medium bedded slightly metamorphosed Orbitolina bearing marly limestone		
0.86	63	7	K_1^{sc}	Yellowish cream and dark grey slightly metamorphosed sandstone, calcareous sandstone, sandy limestone, dolomitic limestone, siltstone and conglomerate		
0.14	27	3	J^q	Alternation dark grey and pink slightly metamorphosed sandstone with quartzitic sandstone in lower part and pale pink quartzite in upper part		
0.71	54	6	Si	Silicic Vein		
0.14	27	3	J^{ms}	Dark grey slightly metamorphosed sandstone with intercalation of pale pink quartzitic sandstone and quartzite		
0.14	27	3	ms, sl	Assemblage undivided dark grey sandstone and slate		
0.50	45	5	J^{sl}	Dark grey slightly metamorphosed slate, phyllite, schist and locally with intercalation of sandstone		
0.86	63	7	mo	Monzodiorite - Monzonite (Post _Early Cretaceous)		
0.86	63	7	mmd	Microdiorite _ Micromonzodiorite (Post _Early Cretaceous)		
0.03	9	1	Q	Recent alluvium		
0.01	0	0	-	Urban Infrastructures		

3.4- Structural data

In order to trace faulted structures of Khondab area, the six Landsat ETM+ bands of 1 to 7 (except the 6th band due to its poor resolution),

are analyzed. Using Optimum Index Factor (OIF) index, the proper RGB combination is defined as 7, 4, 3. As a result of principal component analysis of the RGB map, the first PC is selected due to its high spectral

differences. Directional filters are applied on resulted RGB map of Landsat ETM⁺ in different directions to identify proper direction of faulted structures (Figs. 10 and 11). Regarding well specification of faulted structures, the structures are also mapped using geological map of the study area and then buffered by 1500 meters in five classes (Fig. 12). The two resulted maps of structural features are integrated through OR fuzzy operator and got the weight 8 out of 10 in final fuzzy membership operation (Table 4 and Fig. 13).

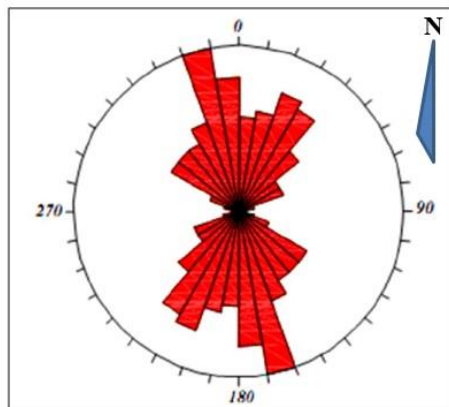


Figure 10) Rose diagram of faulted structures of Khondab area.

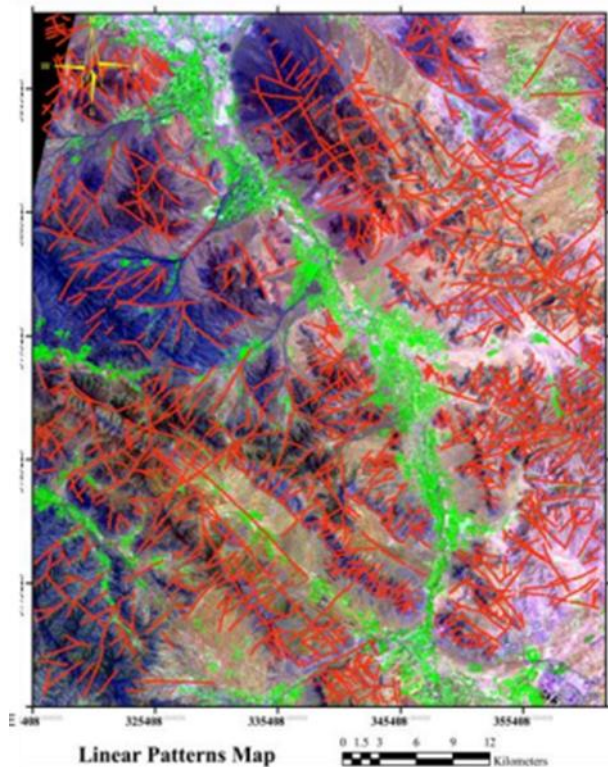


Figure 11) Map of faulted structures of Khondab area.

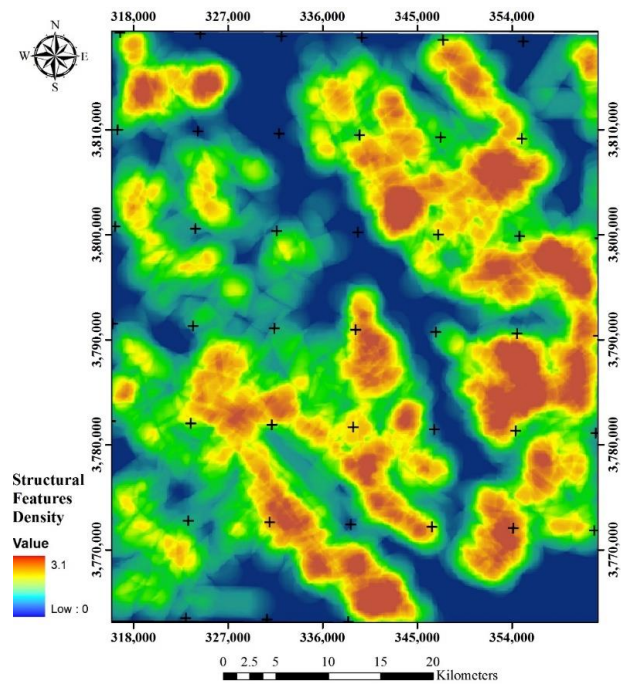


Figure 12) Buffered faulted structures of Khondab area.

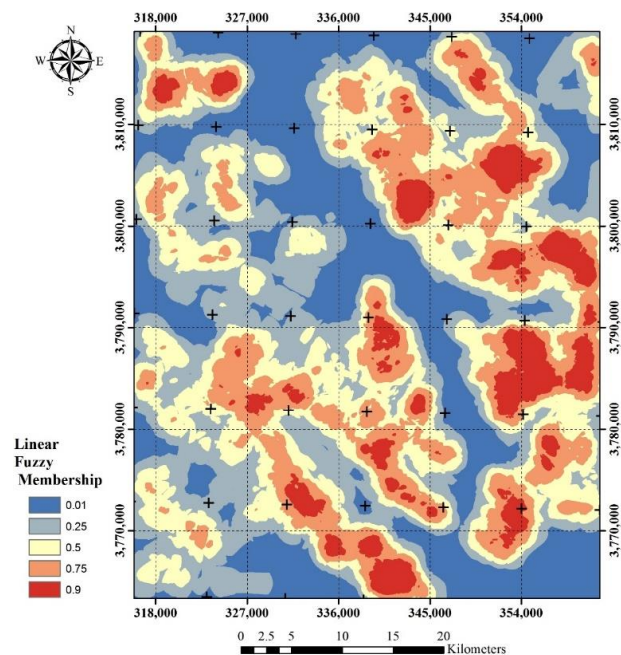


Figure 13) Final weighted map of faulted structures of Khondab area.

3.5- Final fuzzy integration procedure

In this step, fuzzy operators are applied to the fuzzy membership values and final mineral prospectivity map of Khondab area is resulted after converting the output data to non-fuzzy values (Defuzzification) (Fig. 14).

Defuzzification is done according to Gamma membership value of 0.9 associated with surface

measurement plot of the study area (Fig. 15). Based on promising targets and geological features of the area, priority rating exploration map is proposed as it is shown in Figure 16.

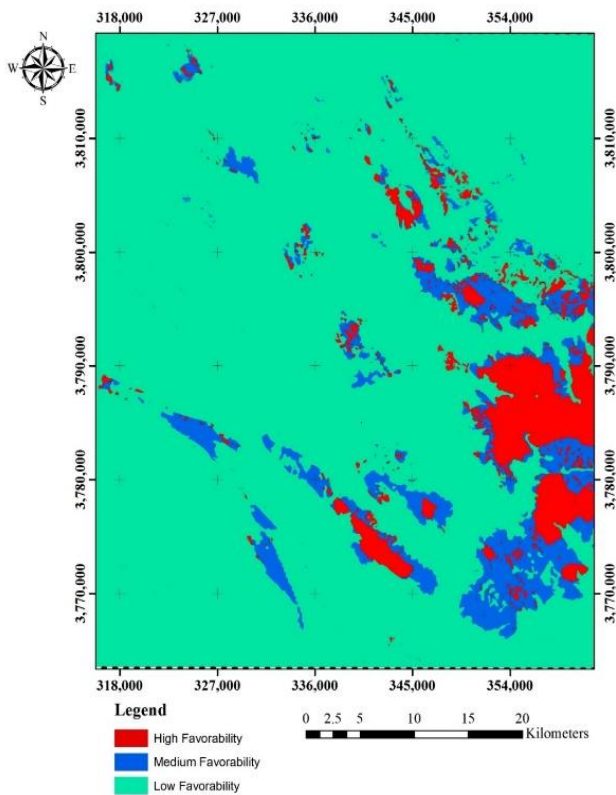


Figure 14) Final defuzzied prospectivity map of Khondab area.

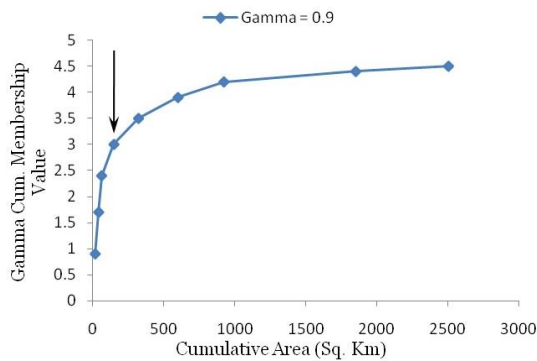


Figure 15) Gamma membership value associated with surface measurement plot of the study area.

3.6- Validation of Fuzzy Logic Integration Modelling

Finally, revealed promising zones of fuzzy logic prospectivity map is compared to previously known mineral occurrences of the study area. Promising regions of the prospectivity map are mostly overlapped by the exposed mineralized zones and previously known deposits of the area (Fig. 17).

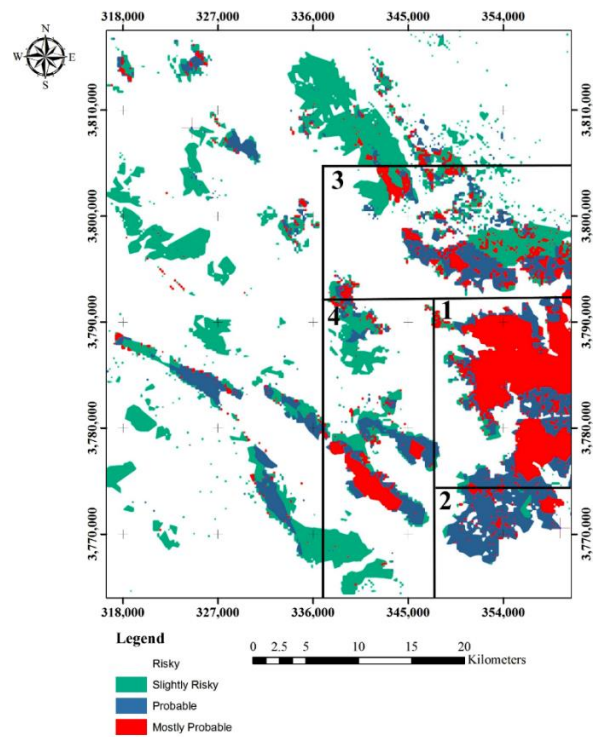


Figure 16) Final prospectivity map of Khondab area. According to priority rating of exploration targets which vary between 1 to 4, the east and the south eastern parts of the study area are the promising parts for further prospectivity of MVT deposits in Khondab area.

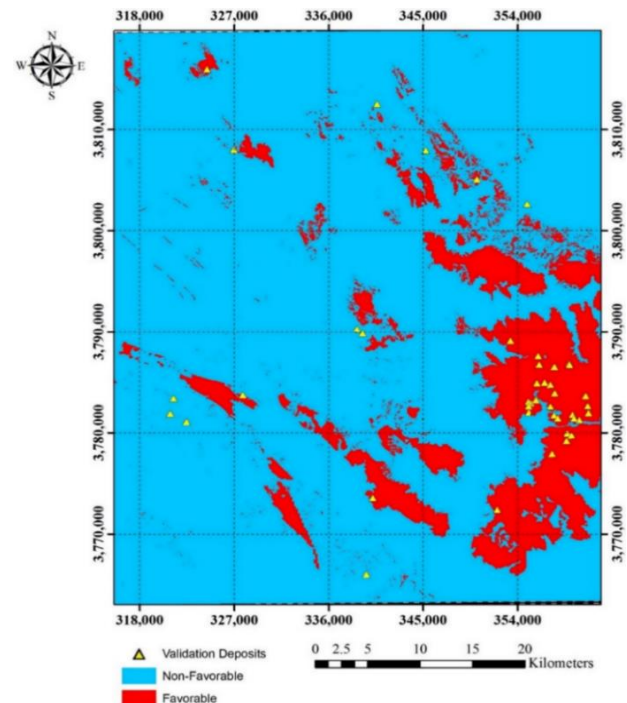


Figure 17) Validation map of fuzzy logic integration modelling. As it is clear in the map, most of the known deposits are overlapped by the resulted promising areas of fuzzy logic data integration technique.

Microscopic studies of the polished thin features of the exposed mineralized zones (Fig. sections also confirmed MVT mineralization 18).

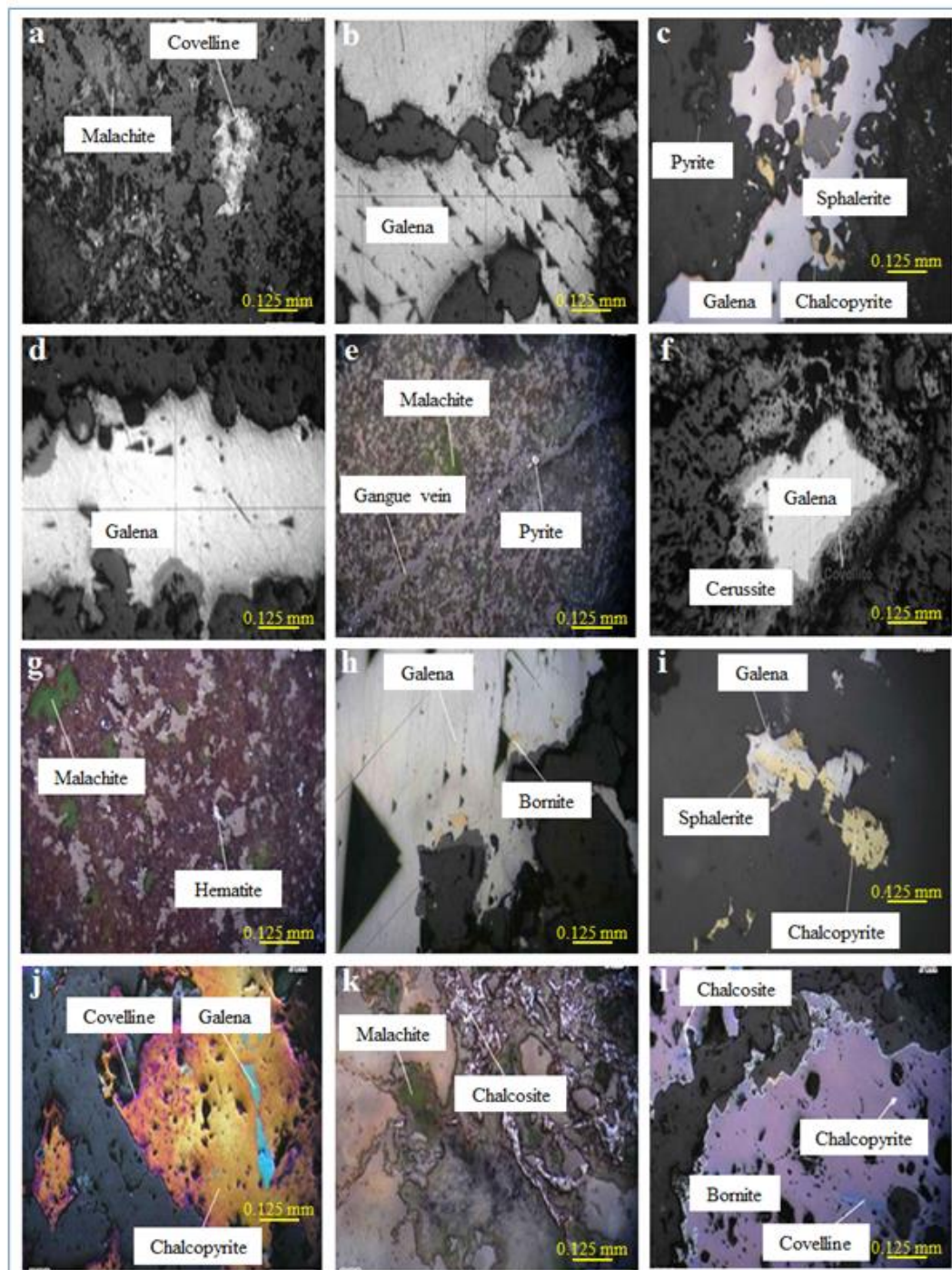


Figure 18) Microscopic images of the collected samples of Khondab area. As it is clear in the pictures, specified minerals are the frequent ones associated with MVT mineralization. (a) Sample Code: CB1P-1-PPL Image at X160 Magnification, (b) Sample Code: ZCT12.P5-PPL Image at X160 Magnification, (c) Sample Code: CB12P-1-PPL Image at X160 Magnification, (d) Sample Code: ZCT13.P8-PPL Image at X160 Magnification, (e) Sample Code: Sample Code: CB1P-3-PPL Image at X160 Magnification, (f) Sample Code: ZCT14.P2-PPL Image at X100 Magnification, (g) Sample Code: CB5-1-PPL Image at X160 Magnification, (h) Sample Code: CB2P-2-PPL Image at X160 Magnification, (i) Sample Code: CB12P-2-PPL Image at X160 Magnification, (j) Sample Code: CT2P-6-PPL Image at X160 Magnification, (k) Sample Code: CB12P-2-PPL Image at X160 Magnification, (l) Sample Code: CB12P-2-PPL Image at X160 Magnification.

Table 2) Detailed information of geophysical layer.

Logistical Fuzzy Membership	Class Score	Class Weight	Class Name	Layer Weight	Evidence Map
0.98	63	9	So High	7	Geophysical Evidence Map
0.88	49	7	High		
0.5	35	5	Medium		
0.12	21	3	Poor		
0.01	7	1	So Poor		

Table 3) Detailed information of the remote sensing layer.

Linear Fuzzy Membership	Class Score	Class Weight	Class Name	Layer Weight	Evidence Map
0.9	54	9	Silicification	6	Alteration Evidence Map
0.7	42	7	Dolomitization		
0.5	30	5	Phyllic		

Table 4) Detailed information of laminated structures.

Linear Fuzzy Membership	Class Score	Class Weight	Class Name	Layer Weight	Evidence Map
0.9	72	9	very high density	8	Faults Density & Structural Features Evidence Map
0.75	64	8	High Density		
0.50	49	7	Medium Density		
0.25	48	6	Low Density		
0.01	40	5	very Low Density		

4- Conclusion

Based on the resulted prospectivity map of fuzzy logic model, the occurrence probability of MVT mineralization in Sanandaj-Sirjan zone is not too high. Processing ETM⁺ satellite imagery data by Crosta transformation technique results in three important hydrothermal alteration zones of silicified, dolomitized and phyllic. The alteration zones are mostly associated with the known MVT mineralized zones of the study area. Resulted map of the fuzzy model is in accordance with field evidences. Validation process indicates that Cretaceous limestone units are in high correlation with MVT mineralization in this area. Based on priority rating of exploration targets, the eastern and the south-eastern parts of the study area are the most promising parts for further exploration of MVT deposits.

References

Adeli, S. 2008. Mineral potential mapping of Chah-Firuzeh copper deposit using GIS.

Unpublished M.Sc. Thesis, University of Tehran, Iran (in Persian).

An, P., Moon, W. M., Rencz, A. 1991. Application of fuzzy set theory for integration of geological, geophysical and remote sensing data. Canadian Journal of Exploration Geophysics: 27, 1–11.

Bonham-Carter, G. F. 1994. Geographic Information Systems Geoscientists: Modeling with GIS. Pergamon, Oxford.

Brown, M. P., Grundy, W. N, Lin, D., Cristianini, N., Sugnet, C.W., Furey, T.S., Ares, M., Haussler, D. 2000. Knowledge-based analysis of microarray gene expression data by using support vector machines. Proceeding National Academy of Science, USA: 97, 262–267.

Carranza, E. J. M., Mangaoang, J. C., Hale, M. 1999. Application of mineral exploration models and GIS to generate mineral potential maps as input for optimum land-use planning in the Philippines. Natural Resources Research: 8, 165–173.

- Carranza, E. J. M., Hale, M. 2001. Geologically Constrained fuzzy mapping of gold mineralization potential, Baguio district, Philippines. *Natural Resources Research*:10,125–136.
- Cheng, Q., Agterberg F. P. 1999. Fuzzy Weights of Evidence Method and its Application in Mineral Potential Mapping. *Natural Resources Research*: 8, 235–242.
- Chung, C. F., Agterberg, F. P. 1980. Regression models for estimating mineral resources from geological map data. *Journal of the International Association for Mathematical Geology*:12, 473–488.
- Eddy, B. G., Bonham-Carter, G. F., Jefferson, C. W. 2006. Mineral potential analyzed and mapped at multiple scales - a modified fuzzy logic method using digital geology. In : J.R. Harris (ed.), *GIS for the Earth Sciences*, Geological Association of Canada: 143–162.
- Eliasi, G. H., 2006. Mineral potential mapping of Now-Chun copper deposit using GIS. Unpublished M.Sc. Thesis, University of Tehran, Iran (in Persian).
- Gettings, M. E., Bultmann, M. W. 1993. Quantifying favorableness for occurrence of a mineral deposit type - an example from Arizona". USGS Open-File Report 93–392, 23.
- Harris, J. R., Wilkinson, L., Heather, K., Fumerton, S., Bernier, M. A., Ayer, J., Dahn, R. 2001. Application of GIS processing techniques for producing mineral prospectivity maps - a case study: Mesothermal Au in the Swayze Greenstone Belt, Ontario, Canada. *Natural Resources Research*: 10, 91–124 .
- Karimi, M., Valadan Zoej, M. J. 2003, Mineral potential mapping of copper minerals with GIS. Commission WG IV/1.
- Nykanen, V., Groves, D I., Ojala, V. J., Eilu, P., Gardoll, S. J., 2008. Reconnaissance scale conceptual fuzzy-logic prospectivity modelling for iron oxide copper-gold deposits in the northern Fennoscandian Shield, Finland. *Australian journal of Earth Sciences*: 55, 25–38.
- Pazand, K., Hezarkhani, A., Ghanbari, Y. 2014. Fuzzy analytical hierarchy process and GIS for predictive Cu porphyry potential mapping: a case study in Ahar –Arasbaran Zone (NW, Iran). *Arabian Journal of Geosciences*: 7, 241–251.
- Pazand, K., Hezarkhani, A. 2018. Predictive Cu porphyry potential mapping using fuzzy modelling in Ahar–Arasbaran zone, Iran. *Journal Geology, Ecology, and Landscapes*, DOI: 10.1080/24749508.2018.1438741
- Porwal, A., Carranza, E. J. M., Hale, M. 2003. Knowledge-driven and data-driven fuzzy models for predictive mineral potential mapping. *Natural Resources Research*: 12, 1–25.
- Rasekh, P., Kiani, F. H., Asadi, H., Tabatabaei, S. H. 2016. Mineral Prospectivity Mapping by Fuzzy Logic Data Integration, Kajan Area in Central Iran. 34th National and the 2nd International Geosciences Congress, Tehran, Iran.
- Reddy, R. K. T., Bonham-Carter, G. F. 1991. A Decision-Tree Approach to Mineral Potential Mapping in Snow Lake Area, Manitoba. *Canadian Journal of Remote Sensing*: 17, 191-200
- Rowan, L. C., Mars, J. 2003. Lithologic Mapping in the Mountain Pass, California Area Using Advanced Spaceborne Thermal Emission and Reflection Radiometer (ASTER) Data. *Remote Sensing of Environment*: 84, 350–366.
- Sameni, M. 2005. Exploration of hydrothermal alterations of Kolahbid exploration area using remote sensing data. Unpublished

M.Sc. Thesis, Islamic Azad University of Mahalat, Iran (in Persian).

Ziaii, M., Pouyan, A., Ziaei M. 2009. A Computational Optimized Extended Model for Mineral Potential mapping Based on WofE Method. *American Journal of Applied Sciences*: 6, 200–203.